Brain, Behavior, and Immunity 101 (2022) 318–332

Contents lists available at ScienceDirect

Brain Behavior and Immunity

journal homepage: www.elsevier.com/locate/ybrbi

Maternal P2X7 receptor inhibition prevents autism-like phenotype in male mouse offspring through the NLRP3-IL-1β pathway

Dorottya Szabó [a,b], Pál Tod [a], Flóra Gölöncsér [a], Viktor Román [c], Balázs Lendvai [c], Lilla Otrokocsi [a,1], Beáta Sperlágh [a,b,*,1]

[a] Laboratory of Molecular Pharmacology, Institute of Experimental Medicine, Budapest, Hungary
[b] János Szentágothai Doctoral School, Semmelweis University, Budapest, Hungary
[c] Department of Pharmacology and Drug Safety Research, Gedeon Richter Plc., Budapest, Hungary

ARTICLE INFO

Keywords:
Autism
Neurodevelopment
Infection
Maternal immune activation
Cytokines
Behavior
Poly(I:C)
Neuroinflammation
P2X7

ABSTRACT

Autism spectrum disorder (ASD) is a complex neurodevelopmental condition caused by interactions of environmental and genetic factors. Recently we showed that activation of the purinergic P2X7 receptors is necessary and sufficient to convert maternal immune activation (MIA) to ASD-like features in male offspring mice. Our aim was to further substantiate these findings and identify downstream signaling pathways coupled to P2X7 upon MIA. Maternal treatment with the NLRP3 antagonist MCC950 and a neutralising IL-1β antibody during pregnancy counteracted the development of autistic characteristics in offspring mice. We also explored time-dependent changes of a widespread cytokine and chemokine profile in maternal blood and fetal brain samples of poly(I:C)/saline-treated dams. MIA-induced increases in plasma IL-1β, RANTES, MCP-1, and fetal brain IL-1β, IL-2, IL-6, MCP-1 concentrations are regulated by the P2X7/NLRP3 pathway. Offspring treatment with the selective P2X7 receptor antagonist JNJ47965567 was effective in the prevention of autism-like behavior in mice using a repeated dosing protocol. Our results highlight that in addition to P2X7, NLRP3, as well as inflammatory cytokines, may also be potential biomarkers and therapeutic targets of social deficits and repetitive behaviors observed in autism spectrum disorder.

1. Introduction

Autism spectrum disorder (ASD) is a pervasive neurodevelopmental disorder caused by genetic and environmental factors. The prevalence of ASD is estimated at 1–2 % worldwide and increasing, the underlying pathology is not fully explored though (Maenner et al., 2020). There is a growing body of evidence that environmental factors during pregnancy play a role in ASD development ranging from perinatal infections (Jiang et al., 2016), maternal autoimmune diseases (Buehler, 2011; Wu et al., 2015), dysbiosis (Hughes et al., 2018), to asthma and adverse perinatal events (Gardener et al., 2009). The common denominator among these conditions is an elevated maternal immune activity level, which has been linked to an enhanced risk of ASD in the offspring (Lyall et al., 2014). During maternal infection, the level of pro-inflammatory cytokines increases in the plasma, which probably transduces temporary and long-lasting changes in fetal neurodevelopment (Goines et al., 2011; Jones et al., 2017).

Purinergic P2X7 receptors are ligand-gated non-selective cation channels expressed by immune cells and intrinsic cells of the CNS. P2X7 activation is well known as an obligatory co-stimulus for the post-translational processing of pro-inflammatory cytokines in peripheral immune cells (Bartlett et al., 2014; Solle et al., 2001). Various external and internal danger signals. i.e. pathogen-associated and damage-associated molecular patterns (PAMPs and DAMPs) can challenge the innate immune system. The primary external danger stimulus, such as bacterial lipopolysaccharide or viral RNA sequence acts on TLR receptors, which leads to the transcription of inflammatory cytokine precursors such as pro-IL-1β or pro-IL-18. Then, a typical DAMP, elevation of extracellular ATP during cellular damage or inflammation activates P2X7, resulting in the formation of active NLRP3 inflammasome (Karmakar et al., 2016; Mariathasan et al., 2006). NLRP3 is a component of the innate immune system that belongs to the NOD-like receptor subfamily of pattern recognition receptors and functions as multimeric protein complex that initiates an inflammatory form of cell

* Corresponding author at: 1083 Budapest, Szigony 43, Hungary.
E-mail address: sperlagh@koki.hu (B. Sperlágh).
[1] Equal contribution.

https://doi.org/10.1016/j.bbi.2022.01.015
Received 23 September 2021; Received in revised form 29 December 2021; Accepted 16 January 2022
Available online 20 January 2022

death and proinflammatory cytokine production (He et al., 2016; Yang et al., 2019). The assembly of inflammasome complexes induces caspase-1 activation (Martinon et al., 2002; Sutterwala et al., 2006). Pro-IL-1β is synthesized as an inactive cytoplasmic precursor that is processed into a biologically active form ready to be released to the extracellular space by caspase-1 (Burns et al., 2003; Dinarello, 2005; Kanneganti et al., 2007; Lamkanfi et al., 2007; Pirhonen et al., 1999; Thomas et al., 2009) in response to various pro-inflammatory stimuli, including viruses or poly(I:C) (Kanneganti et al., 2007; Mariathasan et al., 2006). Therefore, the P2X7-NLRP3 route is one important pathway responsible for the conversion of the innate immune response to inflammation (Di Virgilio et al., 2017). Based on this information, we assumed that NLRP3 and IL-1β might be additional mediators in the effects of P2X7 on neuronal development.

The role of the P2X7 has already been associated with a wide variety of central nervous system disorders (Sperlágh and Illes, 2014). Using the MIA mouse model, we demonstrated that endogenous P2X7 activation is necessary and sufficient to develop an ASD-like phenotype in male offspring. Maternal poly(I:C) (PIC) treatment (4.5 mg/kg) of P2rx7$^{+/+}$ mice evoked autism-like behavioral and histological alterations in offspring, increased ATP, ADP, and IL-6 levels in maternal plasma, elevated ATP and IL-6 levels in fetal brains. Both genetic deletion and a single, one-dose pretreatment with a specific CNS permeable P2X7 antagonist, JNJ47965567, prevented MIA-induced changes and cytokine responses in offspring (Horváth et al., 2019). Moreover, both maternal and offspring treatment with JNJ47965567 was effective in the alleviation of symptoms. However, the exact mechanism whereby activation of P2X7 following MIA leads to ASD symptoms is not yet fully understood. Recently, the involvement of P2X7 was also demonstrated in a genetic model of Rett syndrome in MECP2 $^{308/y}$ mice (Garré et al., 2020). Rett syndrome is a condition that was previously classified as an autism spectrum disorder, but has already been removed from the DSM-5 criteria system (Diagnostic and Statistical Manual of Mental Disorders) as it is characterized by a specific genetic change (American Psychiatric Association, 2017). Mutations in methyl CpG-binding protein 2 (MECP2) cause autism-like symptoms that are similar in appearance, but may differ in severity from ASD, and the social deficit is usually temporary, unlike ASD (Persico et al., 2019).

Aiming to explore the signaling pathways activated by MIA coupled downstream to maternal P2X7 activation, we administered pharmacological treatments to interfere with downstream signaling pathways linking P2X7 activation to behavioral, brain morphological and biochemical abnormalities. As a close associate of P2X7 with NLRP3 and IL-1β is known in the literature, we examined the effect of NLRP3 and IL-1β inhibition in the MIA mouse model, investigating the potential involvement of a well-known inflammatory signaling pathway in the development of ASD-like symptoms. Next, MIA-induced time-dependent changes of inflammatory cytokines and chemokines in the maternal circulation and fetal brain were explored in search of additional potential mediators that may play a role in MIA-induced P2X7-mediated long-term impact on brain development. Detecting the changes in the levels of inflammatory mediators in the maternal plasma may be used in the future as a diagnostic tool to identify the sensitive population and predict the treatment response to drugs targeting the immune system, including P2X7 and NLRP3 antagonists, or to monitor treatment response. Finally, we examined whether the offspring treatment with JNJ47965567 is effective in restoring autism-like features aiming to demonstrate the direct symptom-reducing potential of a repeated dosing protocol, more closely mimicking a potential human administration regime.

2. Materials and methods

2.1. Animals

Maternal immune activation (MIA) model of autism was performed as described in our previous study (Horváth et al., 2019). The animals were kept under standard laboratory conditions in 12 h light–dark cycles, in humidity (60 ± 10%) and temperature (23 ± 2 °C) controlled rooms with food (breeding diet, V1124-000, Sniff Spezialdiäten GmbH) and water provided *ad libitum*. All efforts were taken to minimize animal suffering and reduce the number of animals used. The local Animal Care Committee of the Institute of Experimental Medicine approved all experimental procedures (Permission No: PEI/001/778–6/2015). Experiments were performed on treatment- and test-naïve wild-type P2rx7$^{+/+}$, P2rx7$^{-/-}$ and IL-1αβ$^{-/-}$ mice (Horai et al., 1998). P2rx7$^{-/-}$ and IL-1α/β $^{-/-}$ animals were generated using homologous recombination targeting. The original breeding pairs of P2rx7$^{-/-}$ mice were kindly

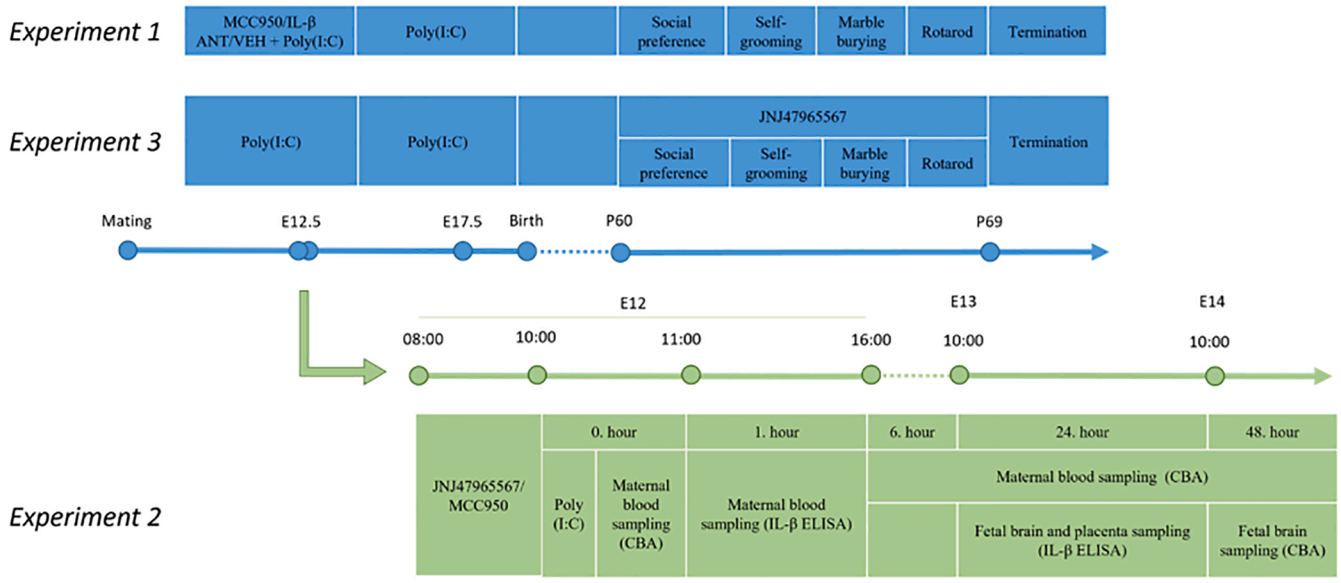

Fig. 1. Experimental design of the study. Timeline of experiments and treatments. In *Experiment 1* and *3*, we examined the ASD-related behaviours following two doses of maternal poly(I:C) treatment at E12.5 and E17.5. Maternal pretreatment (MCC950) was used in *Experiment 1*, and repeated offspring treatment (JNJ47965567) was used in *Experiment 3*. In *Experiment 2*, maternal and fetal tissues were collected after a single-dose poly(I:C) and prior maternal pretreatment (MCC950/JNJ47965567).

supplied by Christopher Gabel from Pfizer, Inc. (Groton CT, USA). The targeting construct was created by RT-PCR using total RNA isolated from rats. The sequences of the primers were as follows: P2X7-F1 (5′-CGGCGTGCGTTTTGACATCCT-3′) and P2X7-R2 (5′-AGGGCCCTGCGGTTCTC-3′) (Solle et al., 2001). Genomic DNA was isolated from the tails of $P2rx7^{+/+}$ and $P2rx7^{-/-}$ animals and the genotypes were confirmed by PCR analysis. Overall nine backcross generations on C57BL/6 were performed for the $P2rx7^{-/-}$ mouse colony used in our experiments. The breeding pairs of IL-1αβ double knockout mice were derived from the Laboratory Animal Research Center (Institute of Medical Science, University of Tokyo). IL-1α targeting construct was created by replacing a 1.5-kb DNA fragment between the Sau3AI and KpnI sites in exon 5 and intron 5 with a lacZ-pA-PGK-hph-pA cassette. A 2.45-kb DNA fragment between the HincII and BstXI sites in exons 3 and 5 was deleted and replaced by a lacZ-pA-PGK-neo-pA cassette for creating the IL-1β targeting vector. IL-1α/β double-KO mice were produced by successive homologous recombinations in the embryonic stem cell.

In each series of experiments, 40–60 adult 10–14 week old females and males (weighing 25–30 g) of the same age and genotype were mated in groups of 2 or 3 randomly assigned regardless of further treatment. Mating occurred once every week in order to follow days of embryonic development. Females were kept in small (approx. 4–6) groups until proven pregnant, while males were kept individually throughout the breeding. Vaginal plugs were investigated in the morning after breeding, and on the day of first treatment (E12.5), the belly size and shape of dams reassured the pregnancies. Pregnant females were randomized into defined experimental groups. Fecundity was reduced to approximately 60% after poly(I:C) treatment and 80% after saline treatment. These spontaneous abortion rates were similar to those reported by other groups using the MIA model (Mueller et al., 2019). Only the male offspring were further tested since the female offspring from the same litters appear mostly resilient to the effects of MIA (Estes et al., 2020). Based on our previous experience, one pregnant dam gives birth to an average of 5 males; therefore, we calculated an ideal sample size prior to breeding process as described in our previous study (Horváth et al., 2019). Experimental animals were transferred from the breeding site to the animal room of the behavioral testing unit one week before the planned behavioral tests. Sample sizes of the groups may show variance due to high-variance spontaneous miscarriages, maternal and neonatal deaths among treated animals.

2.2. Treatments

To induce MIA, pregnant dams were challenged with 3 mg/kg dose of poly(I:C) (Sigma-Aldrich, P9582, LOT#118M4035V, LOT#12190304) or physiological saline intraperitoneal injection on E12.5 and 1.5 mg/kg of poly(I:C) on E17.5 in each experiment, as in our previous study (Horváth et al., 2019) (Fig. 1). In Experiment 1, a cohort of pregnant dams was pretreated with 50 mg/kg of NLRP3 selective antagonist MCC950 (CRID3 sodium salt, Tocris Bioscience, Cat. No. 5479) or with 25 μg/kg goat anti-mouse IL-1 beta /IL-1F2 antigen affinity-purified polyclonal IgG (R&D Systems, AF-401-NA) on E12.5, two hours before poly(I:C) injection. Controls received the same volume (100 μL) of saline injection at the same time. MCC950 exerts its effect by closing the active conformation of NLRP3 to the inactive state and directly interacting with the Walker B motif within the NLRP3 NACHT domain, according to the manufacturer's datasheet. In *Experiment 2*, two cohorts of pregnant mice received JNJ47965567 (30 mg/kg, Tocris Bioscience) or 50 mg/kg MCC950 two hours prior to MIA induction, while control groups received an equivalent amount of the vehicle (30% Captisol solution: sulfobutylether-7β-cyclodextrin, Sigma-Aldrich or physiological saline, respectively). In Experiment 3, offspring mice received 20 mg/kg/day P2X7 antagonist JNJ47965567 or equivalent amount of Captisol solution intraperitoneal injection for nine days, with a total of 9 injections administered in the morning, 2 h before the start of the behavioral test.

2.3. Experimental design

In *Experiment 1* and *Experiment 3,* behavioral tests were performed on male offspring at 8–10 weeks of age by an experimenter blinded to the treatments in the following order: social preference, self-grooming, marble burying, rotarod test. Then animals were sacrificed, and samples were collected for morphology analyses. In *Experiment 2*, we collected plasma samples from tail veins of pregnant mice on E12 day at 0, or in some experiments, 1, 6, and 24 h following poly(I:C) injection. At 24 or 48 h, mice were anesthetized by constantly administered isoflurane, while maternal plasma, fetal brain, and placental samples were collected for enzyme-linked immunoassay or cytometric bead array analyses, then dams were terminated by cervical dislocation. All tests were evaluated automatically or by a blind method. All animal-contact devices used for behavioral testing were cleaned with 20% alcohol and then water after each test animal to reduce odors.

2.4. Social preference test

We used the methodology of Naviaux (Naviaux et al., 2013) in a three-chamber plexiglass arena (60x40x33 cm) with one wire cage placed in each side chamber. The experiments consisted of two phases of 5 min habituation and 10 min test phase. During the first habituation phase, the test animal was free to explore the entire arena for 5 min. The mouse was then confined to the middle chamber of the arena, and a stranger mouse of the same age and sex was placed into a wire cage of one side of the chamber. The other cage on the other side chamber remained empty. Then the doors were opened between the cages at the beginning of the 10-minute test phase. Live tracking measurements were performed with Noldus Ethovision XT 13 software (Wageningen, the Netherlands), comparing the time the test mouse spent in each of the sniffing zones determined in the software. Social preference was expressed in percentage as cumulative duration (seconds) spent in the empty or intruder sniffing zone divided by the time spent in both sniffing zones multiplied by 100.

2.5. Self-grooming test

The self-grooming test was performed as described by Kyzar (Kyzar et al., 2011). Before experiments, mice were habituated to the experimental room for 30 min. Animals were individually placed into glass observation cylinders (12 cm diameter, 20 cm height), and their spontaneous novelty-evoked grooming behavior was recorded for 10 min. Grooming behavior was manually scored using Noldus Observer XT software (Wageningen, the Netherlands), and the cumulative duration of self-grooming in seconds was expressed.

2.6. Marble burying test

Marble burying test was designed based on a study by Malkova (Malkova et al., 2012). On the surface of 4–5 cm thick, clean bedding, 20 marbles were placed equidistantly arranged in 4x5 rows in clean animal cages (36.7 × 14.0 × 20.7 cm). 1/3 surface remained free from marbles where the mice were gently placed, and the cage was covered by plexiglass for the 10 min testing period. Marbles covered by > 60% bedding were considered buried.

2.7. Rotarod test

The rotarod test was performed according to (Naviaux et al., 2013) on a rotarod apparatus (Rotarod Treadmill 755, IITC Life Science, California, United States). Mice were gently placed onto a rod that can rotate at a constant or accelerating speed. The instrument enables the simultaneous examination of 5 mice. Each mouse underwent training on

two consecutive days at a constant 4 rpm speed to achieve the ability to balance on the rod for at least 30 s. During testing, the rod was accelerating evenly from 4 to 40 rpm in 5 min. Latency to fall was measured four times a day on two consecutive days expressed in seconds. The intertrial interval was at least 30 min.

2.8. Quantitative immunohistochemistry

Immunohistochemical staining was performed on the cerebellum of 6 to 13 animals per group to quantify the number of Purkinje cells. Mice were anesthetized with gradual CO_2 inhalation and perfused with 4% paraformaldehyde (PFA). Brains were removed and postfixed overnight in 4% PFA. Samples were rinsed three times with PBS, and 50 μm parasagittal sections were cut from the cerebellum using a Leica vibratome (Buffalo Grove, IL, United States). Sections were permeabilized in blocking solution containing 5% normal horse serum, 1% bovine serum albumin (BSA), and 0.3% Triton X-100 in 0.1 M phosphate buffer (PB) for 2 h at room temperature. Sections were incubated overnight at 4 °C with primary antibodies: anti-calbindin antibody (Swant, CB-38a, 1:12,000). Then we washed the sections three times with PBS again and incubated them for 2 h at room temperature with fluorescent secondary antibody (Alexa-Fluor 488 goat anti-rabbit IgG, 1:3000, Invitrogen). Sections were washed and gently placed onto slides. Drawn samples were covered with a fluorescent staining protective medium and cover slides. Images were taken from the VIIth lobule of the cerebellum (Hashimoto et al., 1995) by a confocal Nikon C2 microscope at 20x magnification. Cell density was calculated manually and using ImageJ software (NIH, Bethesda, MD, United States). The number of Purkinje cells fluorescently labeled in the images was compared to the measured length of the lobule. The Purkinje cell density was expressed in cells/mm.

2.9. Synaptosome integrity analysis using electron microscopy

Whole-brain synaptosome fractions were prepared following the protocol of Köfalvi et al. (2003). After decapitation, brains were homogenized in sucrose-HEPES solution (0.32 M sucrose, 0.01 M HEPES free acid, 0.63 mM Na_2EDTA, pH 7.4) at 4 °C and centrifuged at 3000 g for 5 min. The supernatant was centrifuged at 13,000 g (10 min, 4 °C) in a clean centrifuge tube. The supernatant was then discarded and the P2 pellet was taken up in 45% (v/v) Percoll-Krebs solution (Krebs: 113 mM NaCl, 3 mM KCl, 1.2 mM KH_2PO_4, 1.2 mM $MgSO_4$, 2.5 mM $CaCl_2$, 25 mM $NaHCO_3$, 5.5 mM glucose, 1.5 mM HEPES, pH 7.4) and centrifuged at 13,000*g* for 2 min at 4 °C. The Percoll solution was aspirated from under the synaptosome-rich layer on top of the liquid column, and the remaining synaptosome fraction was removed and recentrifuged at 13,000*g* for 2 min in an equal volume of Krebs solution. The resulting pellet was resuspended twice in Krebs solution, centrifuged, then the supernatant was aspirated. The pellet containing synaptosomes was fixed with 4% paraformaldehyde (pH 7.4) for at least one hour. After rinsing with PBS buffer, it was post-fixed with 1% OsO_4 at room temperature for 30 min. The preparation was stained *en bloc* with 1% uranyl acetate in 50% ethanol (30 min) and dehydrated with 50%, 70%, 90%, 100% alcohol series. Finally, samples were embedded in Taab 812 resin (Taab Laboratories, Aldermaston, UK). Overnight polymerization of samples at 60 °C was followed by ultrathin sectioning using Leica EM UC7 ultramicrotome (Leica Microsystem) and examined with a Hitachi 7100 electron microscope (Hitachi Ltd., Japan) equipped with a Veleta 2 k × 2 k MegaPixel TEM CCD camera (Olympus, Bethlehem, PA, United States). Electron micrographs were taken at 25,000 magnification in all investigated groups. The obtained images were analyzed using "Adobe Photoshop CS3" and "Image J" software. Intact and malformed (uneven membranes, irregular postsynaptic density) synaptosomes were counted manually twice by an investigator blinded to the treatments.

2.10. Quantitative analysis of IL-1β using sandwich enzyme-linked immunoassay technique

Maternal plasma, fetal brain, and placenta IL-1β levels were measured by The Quantikine® Mouse IL-1 beta Immunoassay, R&D Systems (Minneapolis, MN, United States. Plasma samples were collected from vena cava inferior 1 h following intraperitoneal injection of poly(I:C) (3 mg/kg) or saline. Fetal brain and placenta samples were collected 24 h following treatment from pregnant mice that were not used previously for plasma sampling. For homogenisation, samples were placed in lysis buffer (50 mM Tris HCL, 150 mM NaCl, 5 mM $CaCl_2$, 0,02%NaN_2, 1% Triton X-100, pH = 7,4) with 0.1% protease inhibitor double-diluted in PBS. After homogenization and centrifugation, brain homogenate and plasma samples were stored at −80 °C. IL-1β concentration was determined by mouse IL-1β-specific monoclonal antibody pre-coated microplates following the manufacturer's instructions. We determined the optical density with a microplate reader at 450 nm (Cytation™5 Cell Imaging Multi-Mode Reader). We calculated concentration values (pg/ml) using GraphPad (San Diego, CA, United States). For measuring total protein level in tissue samples, absorbance was measured at 560 nm. Fetal brain and placental IL-1β concentrations were expressed in pg/mg protein. Plasma cytokine concentrations were expressed in pg/ml. As specified in the product datasheet, the minimum detectable dose (MDD) of mouse IL-1β ranged from 0.46 to 4.80 pg/mL, the mean MDD was 2.31 pg/mL. Values lower than this were taken as zero.

2.11. Maternal plasma and fetal brain cytokine and chemokine analyses

Maternal plasma samples were collected from the tail vein 0, 6, and 24 h after intraperitoneal injection of poly(I:C) (3 mg/kg) or saline. At 48 h, blood from vena cava inferior and fetal brains were collected and placed into ice-cooled physiological saline. After homogenization and centrifugation, brain homogenate and plasma samples were stored at −80 °C. After careful thawing, the following cytokines and chemokines were measured by multiplex CBA analysis (BD FACSVerse flow cytometer, BD Biosciences): IFN-γ, IL-6, IL-2, IL-4, IL-10, TNF-α, G-CSF, RANTES, MCP-1. FCAP Array 5 (Soft Flow) was used for analysis. Brain cytokine concentration was normalized to total protein level with BCA Protein Assay Kit (Thermo Fisher Scientific, Pierce). Absorbance was measured at 560 nm using a Cytation ™ 5 Cell Imaging Multi-Mode Reader. Fetal brain cytokine concentrations were expressed in pg/mg protein. Plasma cytokine concentrations were expressed in pg/ml.

2.12. Statistics

GraphPad Prism 7 (GraphPad Software) and Statistica 13 (Dell) were used for statistical analyses. Data normality was examined by the Kolmogorov-Smirnov test, where data was logarithmically transformed if necessary. Possible outlier values were detected by the ROUT method (q = 1%) (Motulsky and Brown, 2006), and these data were omitted from the analysis. Data were presented as mean ± s.e.m. of *n* of experiment, where *n* represented the number of animals. Each experiment was repeated in 3–7 independent litters. Data on behavior tests and cytokine concentrations were analyzed by one- and two-way ANOVA with Tukey's post hoc test. Nonparametric ANOVA (Kruskal-Wallis) test completed with Dunn's multiple comparison was used for non-normally distributed data. Data were considered statistically significant if $p < 0.05$. For detailed statistical tests of all experiments, n and p values are provided in the Supplementary Information.

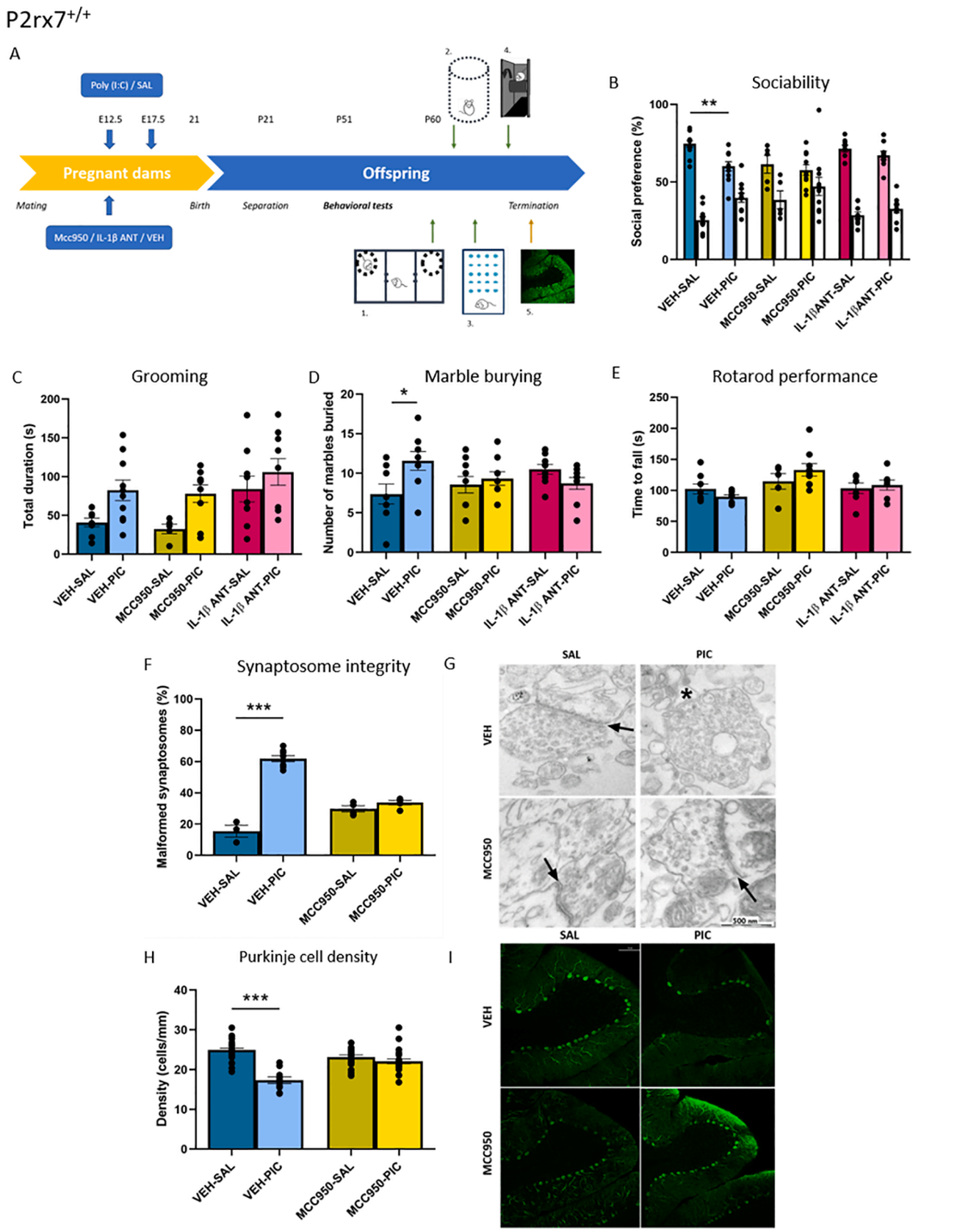

(caption on next page)

Fig. 2. Both maternal NLRP3 (MCC950) and IL-1β antagonist treatment prevented the appearance of certain autistic features in mice. (A) The experimental protocol shown in a flowchart *(Experiment 1)*. (B-E) MIA elicited social deficit (B), increased the time spent burying marbles (D) in VEH treated mice, whereas no effect of poly (I:C) (PIC) was observed in MCC950 and IL-1β antagonist pretreated mice, although both MCC950 treated groups displayed lower social preference compared to VEH-SAL treated group (B). Poly(I:C) treatment slightly increased grooming time; however, the difference did not reach the limit of significance in either group (C). Social preference (%) was calculated as 100 multiplied by the time the test mouse spent interacting with the stranger mouse divided by the total time a test mouse spent with the stranger and the empty cage. The white bars in Figure B show a similarly calculated percentage of time spent sniffing the empty cage. (F-G) Each dot on the diagram represents the ratio of damaged synaptosomes from one brain sample (F). Representative EM image of synaptosome preparations (G). The significant difference in the ratio of malformed synaptosomes of VEH treated whole brain samples had been inhibited by MCC950 treatment. Malformed synapses (asterisk) showed different structures (uneven membranes, irregular postsynaptic densities) from normally developed synapses (arrows). (H-I) Representative image of calbindin-labeled Purkinje cells in lobule VII of the cerebellum. Purkinje cell density decreased by MIA in VEH treated group and was prevented in MCC950-PIC treated group. Data show 10–30 technical replicates in $n = 3$ or 4 animals per group. Scale bar: 100 μm. All data are expressed as mean ± s.e.m. Statistical tests used with exact n, F, and p values are provided in *Supplementary Table*. $^{*}p < 0.05$. $^{**}p < 0.01$. $^{***}p < 0.001$.

3. Results

3.1. Inhibition of NLRP3 and neutralisation of IL-1β alleviate MIA-induced autism-like phenotype

In *Experiment 1*, we examined whether pharmacological blockade of NLRP3 modifies the development of autism-like phenotype in response to MIA. Maternal poly(I:C) treatment reproduced autistic-like elements in the P2rx7$^{+/+}$ offspring, i.e. social deficit (Fig. 2B) and repetitive behavior in marble burying test (Fig. 2D), but did not change self-grooming or sensorimotor coordination (Fig. 2C, E). Maternal pretreatment with NLRP3 antagonist MCC950 (50 mg/kg. i.p.) prevented this phenotype in sociability and marble burying tests (Fig. 2B, D). Similarly, maternal pretreatment with neutralizing IL-1β antibody (25 μg/kg i.p.) prevented the development of social deficit (Fig. 2B) as well as change in repetitive behavior of the offspring (Fig. 2D). Similarly, IL-1α/β-deficient mice did not develop an autism-like phenotype following maternal poly(I:C) treatment (Suppl. Fig. 1). Next, we examined synaptosome integrity and Purkinje cell density. Poly(I:C) treatment impaired synaptosome integrity resulting in a higher percentage of malformed synaptosomes (Fig. 2F-G) and created Purkinje cell loss in the cerebellar VIIth lobe (Fig. 2H-I), while in MCC950 pretreated groups difference in morphology was not detected. Confirming our previous data (Horváth et al., 2019), VEH-SAL and VEH-PIC treated P2rx7$^{-/-}$ mice did not display any aspects of autistic phenotype either in behavior or in morphological hallmarks (Fig. 3B-H). Likewise, maternal MCC950 pretreatment did not affect social or repetitive behaviors (Fig. 3B-D), or aspects of motor coordination (Fig. 3E-H) in this genotype. These data support that activation of NLRP3, inhibited by MCC950, is under the control of P2rx7 activation.

3.2. P2rx7 deficiency and NLRP3 inhibition abrogated poly(I:C) induced elevation in the level of IL-1β in placenta and fetal brain samples

Previous experiments indicated that IL-1β might play a role in converting MIA to offspring autism-like phenotype. In *Experiment 2*, we performed a mouse-specific IL-1β immunoassay to determine whether maternal poly(I:C) induces IL-1β elevation in the maternal circulation, placenta, and offspring brain in wild-type and P2rx7-deficient mice as well as following maternal pretreatment with the selective P2X7 receptor antagonist JNJ47965567 or the NLRP3 inhibitor MCC950. JNJ47965567, MCC950 and its vehicle were administered two hours before the respective poly(I:C) treatment. In P2rx7$^{+/+}$ mice, poly(I:C) increased IL-1β level in maternal plasma as early as 1 h following injection, while the differences detected in plasma samples of P2rx7$^{-/-}$ and JNJ47965567 pretreated mice were not significant (Fig. 4B).IL-1β protein was induced by poly(I:C) in wild-type mice 24 h after injection in placenta (Fig. 4C) and fetal brain (Fig. 4D). P2rx7 gene deficiency and maternal treatment with the selective P2X7 antagonist JNJ47965567 prevented poly(I:C) induced elevation of IL-1β in both tissue types (Fig. 4C-D). The NLRP3 inhibitor MCC950 (50 mg/kg) applied 2 h before maternal poly(I:C) treatment in wild-type mice prevented IL-1β production in the placenta and fetal brain (Fig. 5C-D), whereas an identical treatment did not alter the poly(I:C)-induced difference in IL-1β levels observed in maternal plasma, when compared to saline treatment (Fig. 5B).

3.3. Poly(I:C) induced pro-inflammatory shift in cytokine and chemokine levels in maternal plasma and fetal brain samples

In *Experiment 2*, we also examined the effects of MIA on a wide variety of cytokines and chemokines at different time points (0, 6, 24, and 48 h after MIA) using maternal plasma and fetal brain samples of P2rx7$^{+/+}$ and P2rx7$^{-/-}$ mice (Fig. 6., Suppl.Fig. 1).

In our previous study (Horváth et al., 2019), IL-6 was strongly induced in maternal plasma 2 h after poly(I:C) injection in P2rx7$^{+/+}$ samples, and deficiency of P2rx7 prevented this elevation. Here we examined cytokine concentrations at later time points, 6 h following MIA induction. We found significant IL-6 elevation induced by poly(I:C) in both genotypes indicating the involvement of a P2X7-independent mechanism (Fig. 6B). Plasma RANTES was robustly elevated at 6 h, and the magnitude of the elevation appears to be P2X7-dependent as the increase was significantly smaller in the P2rx7-deficient group. This trend could also be observed at 24 h (Fig. 6F). G-CSF was elevated in both genotypes following MIA induction at 6 h but reduced at 24 h in the P2rx7$^{+/+}$ group. However, the poly(I:C)-induced elevation persisted at 24 and 48 h in the P2rx7$^{-/-}$ mice (Fig. 6D). MIA induced a genotype-independent increase in plasma levels of MCP-1 after poly(I:C) treatment peaking at 6 h. P2X7 deficiency had some effect on the sustained MCP-1 elevation in maternal plasma at 24 h (Fig. 6E). Interestingly, plasma TNF-α showed a significant increase only in the P2rx7$^{-/-}$ group at 6 h (Sup. Fig. 1A). IL-4 levels were unaffected by poly(I:C) treatment in the P2rx7$^{+/+}$ group and were undetectable in P2rx7$^{-/-}$ mice. In case of the IL-4 level by CBA measurement, the theoretical limit of detection is 0.3 pg/mL. thus, most of the P2rx7$^{-/-}$ samples presumably fell below the detection limit. (Fig. 6G). IL-2 was unaffected by the poly(I:C) treatment and was also undetectable in P2rx7$^{-/-}$ mice. The theoretical limit of detection is 0.2 pg/mL in the case of IL-2. No genotype or treatment-related differences were detected in maternal plasma levels of IFN-γ (Supp. Fig. 1A) and IL-10 (Supp. Fig. 1C) at either time point. In fetal brains, poly(I:C) induced a genotype-dependent significant elevation in IL-6 (Fig. 7A), IL-2 (Fig. 7B), and MCP-1 (Fig. 7C) levels compared to the saline-treated group 24 h after the maternal immune activation, which was not observed in samples of P2rx7$^{-/-}$ animals. For IFN-γ (Supp. Fig. 1D), TNF-α (Sup.Fig. 1E), and IL-10 (Supp. Fig. 1F), cytokine levels remained below the detection limit in the P2rx7-deficient group, whereas they were detectable in samples from wild-type animals. Treatment and genotype did not induce significant differences in RANTES (Fig. 7D) and G-CSF (Fig. 7E) levels, although RANTES concentration was significantly increased by poly(I:C) in P2rx7$^{-/-}$ group. While IL-4 concentrations showed very low values in both treatment groups of wild-type animals, much higher values were obtained in P2rx7$^{-/-}$ mice in contrast to its plasma level (Fig. 7F).

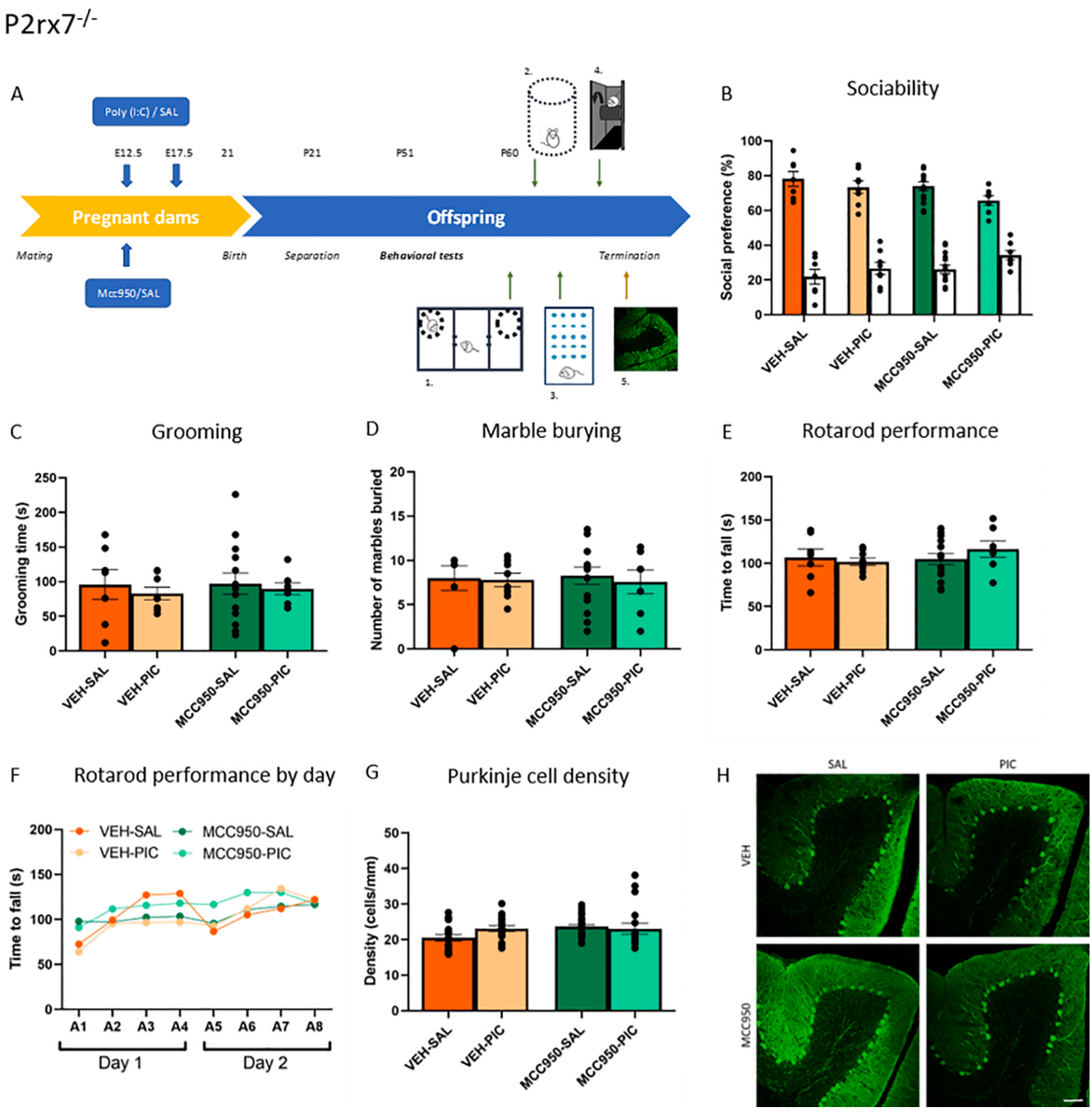

Fig. 3. Maternal poly(I:C) treatment did not elicit autism-like phenotype in either VEH or MCC950 treated P2rx7$^{-/-}$ animals. (A) The experimental protocol shown in a flowchart *(Experiment 1)*. (B) No social deficit appeared in either group. (C-F) Repetitive behaviors (C-D) and sensorimotor coordination (E-F) showed no difference by MIA in either PIC group compared to the control groups. Corresponding to this, no difference appeared in the density of Purkinje cells in lobule VII (G-H). Scale bar 100 μm. All data are expressed as mean ± s.e.m. Statistical tests used with exact n, F, and p values are provided in *Supplementary Table.* $^{*}p < 0.05$. $^{**}p < 0.01$. $^{***}p < 0.001$.

3.4. Repeated offspring treatment with P2X7 antagonist (JNJ47965567) reversed MIA-induced effects in P2rx7 $^{+/+}$ mice

We previously showed that genetic deletion and pharmacological inhibition of offspring P2X7 by a single JNJ47965567 antagonist injection prevented MIA-induced offspring behavioral and histological changes and cytokine responses (Horváth et al., 2019). To further validate P2X7 as a potential drug target, we applied repeated treatment with JNJ47965567 in the same MIA model, which is more similar to a potential human therapeutic treatment period. In *Experiment 3,* JNJ47965567 was administered to offspring at 20 mg/kg/day intraperitoneally, starting from P65 for nine days 2 h before the respective behavior tests.

In the social preference test, MIA resulted in a mild social deficit in VEH treated groups, while offspring treated with JNJ47965567 showed no significant difference regarding maternal treatment indicating the P2X7 antagonist reversed the effect of maternal poly(I:C) (Fig. 8B). In VEH treated groups, MIA significantly increased repetitive behaviors, as total duration of self-grooming and number of buried marbles (Fig. 8C-D) compared to control offspring, while JNJ47965567 administration reversed maternal poly(I:C) effects.

In our previous report (Horváth et al., 2019), we showed MIA caused

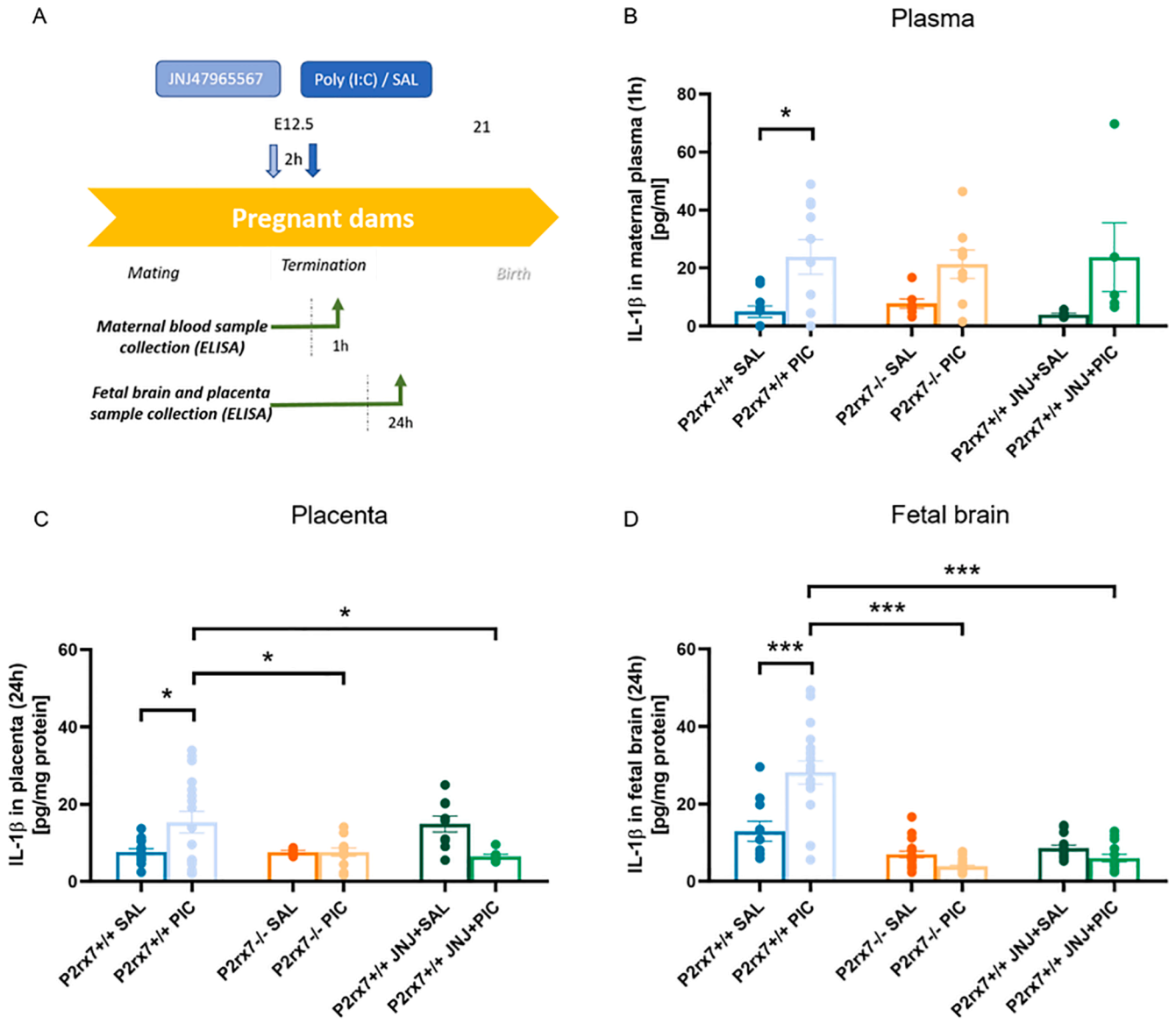

Fig. 4. Poly(I:C) induced elevation in the level of IL-1β in maternal and fetal tissue samples of WT mice. Genetic and pharmacological inhibition of P2X7s prevented significant IL-1β elevation by poly(I:C) in all three tissue types. (A) The experimental protocol shown in a flowchart *(Experiment 2)*. (B) PIC significantly increased the level of pro-inflammatory IL-1β in maternal plasma of P2rx7$^{+/+}$ mice 1 h following PIC injection, but not significantly in samples derived from genetically and pharmacologically P2rx7-deficient mice (B). Plasma samples were collected 1 h following drug administration. Different dots correspond to samples of different animals (5–10 animals per group). (C-D*)* PIC induced elevation in IL-1β concentrations 24 h after MIA induction in placental (C) and fetal brain (D) samples of wild-type mice, while this effect was not observed in samples from P2rx7$^{-/-}$ and JNJ47965567 pretreated P2rx7$^{+/+}$ mice. Two intact placenta and 2–3 fetal brain samples of similar size and different uterine locations were collected from a pregnant animal, so we had 9–17 placenta and 10–24 fetal brain replicates per group, which belonged to 5–9 animals. Cytokine and chemokine values measured in the plasma are expressed in picograms per milliliter, in the fetal brains, and placenta in picograms per mg of total protein. All data are expressed as mean ± s.e.m. Statistical tests used with exact n, F, and p values are provided in *Supplementary Table.* *$p < 0.05$. **$p < 0.01$. ***$p < 0.001$.

impairments in sensorimotor coordination measured by the accelerating rotarod test. However, in this series of experiments decrease in sensorimotor coordination was not observed in offspring (Fig. 8E). Synaptosome integrity was evaluated by electron microscopy. MIA significantly increased the number of abnormally structured synapses in VEH-treated offspring (Fig. 8F-G). On the contrary, repeated JNJ47965567 administration in offspring significantly reduced the number of abnormal synapses. Similar to the rotarod test, Purkinje cell loss after MIA was not observed in this series of experiments (Fig. 8H-I). JNJ47965567 alone had no significant effect on phenotype in any tests.

4. Discussion

In the present study, our primary goal was to identify downstream signaling pathways following P2X7 activation in the MIA mouse model of ASD.

Given the pivotal role of NLRP3 in the innate immune response and its involvement in P2X7 mediated actions, NLRP3 was our first candidate and maternal pretreatment with its selective antagonist MCC950 inhibited the ASD phenotype triggered by MIA. These findings verify NLRP3 inflammasome involvement in the offspring response to MIA. Supporting our data, elevated inflammasome and NLRP3 activations in ASD were observed in a human study (Saresella et al., 2016). NLRP3 may also have a connecting role in the gut microbiome-brain axis,

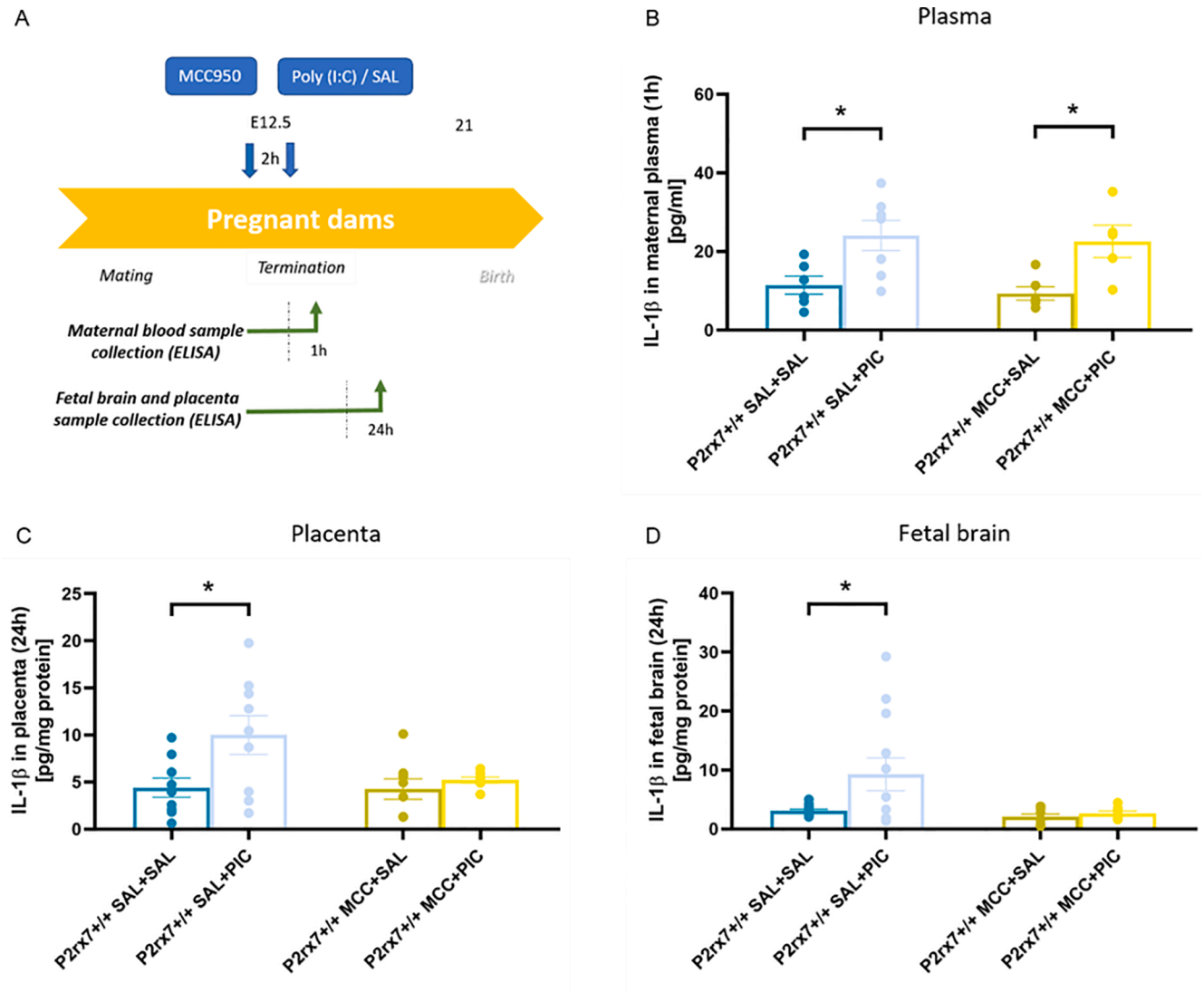

Fig. 5. Pharmacological inhibition of NLRP3 prevented significant IL-1β elevation by poly(I:C) in placenta and fetal brain samples. (A) The experimental protocol shown in a flowchart *(Experiment 2)*. (B) PIC repeatedly increased the IL-1β level in maternal plasma of P2rx7$^{+/+}$ mice 1 h following PIC injection both in NLRP3 antagonist pretreated and saline-treated mice (B). Different dots correspond to samples of different animals (5–10 animals per group). (C-D) PIC also induced elevation in IL-1β concentrations 24 h after MIA induction in placental (C) and fetal brain (D) samples of wild-type mice, while MCC950-pretreated mice showed no significant elevation following poly(I:C) administration. 2 intact placenta and 2–3 fetal brain samples of similar size and different uterine locations were collected from 5 pregnant animals per group. Cytokine and chemokine values measured in the plasma are expressed in picograms per milliliter, in the fetal brains, and placenta in picograms per mg of total protein. All data are expressed as mean ± s.e.m. Statistical tests used with exact n, F, and p values are provided in *Supplementary Table.* $^{*}p < 0.05$. $^{**}p < 0.01$. $^{***}p < 0.001$.

altering the gut microbiota composition eliciting a shift towards a pro-inflammatory phenotype (Hirota et al., 2011; Pellegrini et al., 2020). In P2rx7$^{-/-}$ mice, maternal poly(I:C) did not affect offspring behavior regardless of MCC950, indicating NLRP3 activation is under the regulation of P2X7.

Several studies refer to MIA leading to elevated inflammatory cytokine (Ashwood et al., 2011a; Wong and Hoeffer, 2018) and chemokine levels (Arrode-Brusés and Brusés, 2012; Ashwood et al., 2011b). Based on previous studies, P2X7 provides a co-stimulus posttranslational processing and subsequent cytokine release following a priming endotoxin challenge (Di Virgilio et al., 2017). Therefore, it is reasonable to assume that in MIA model, P2X7-related regulation of offspring response might also be mediated by circulating or local cytokines. Thus, to get a more detailed, time-dependent insight into MIA-induced cytokine response, we collected maternal plasma, placenta, and fetal brain samples at different time points following poly(I:C) challenge. There are many studies on the level of pro-inflammatory and anti-inflammatory cytokines in humans, which might play a role in the pathophysiological mechanism of ASD (Xu et al., 2015).

Elevated IL-6 levels are characteristic of individuals with autism (Li et al., 2009; Masi et al., 2015; Wei et al., 2013). In mice, IL-6 induced in maternal serum can cross the placenta (Wu et al., 2017) and trigger changes in placental physiology and fetal brain (Smith et al., 2007; Zaretsky et al., 2004). In our experiments, pro-inflammatory IL-6 was induced in maternal blood 6 h after poly(I:C) treatment, and IL-6 elevation decreased gradually during the following period. While the increase in IL-6 level after two hours of injection was demonstrated to be P2X7-dependent in our previous study, by the 6th hour another, P2X7-independent mechanism was responsible for the increased IL-6 concentrations in P2rx7$^{-/-}$ animals. Several interrelated signaling pathways can lead to increased IL-6 expression, including IL-1β, TLR3, TLR4, and TNFR1-mediated processes such as TAK-1-IKK-NFKb, or TAK-1-MKK-p38-AP-1 signaling cascades (Adhikari et al., 2007; Ermolaeva et al., 2008). It is possible that cytokines interacted to activate IL-6

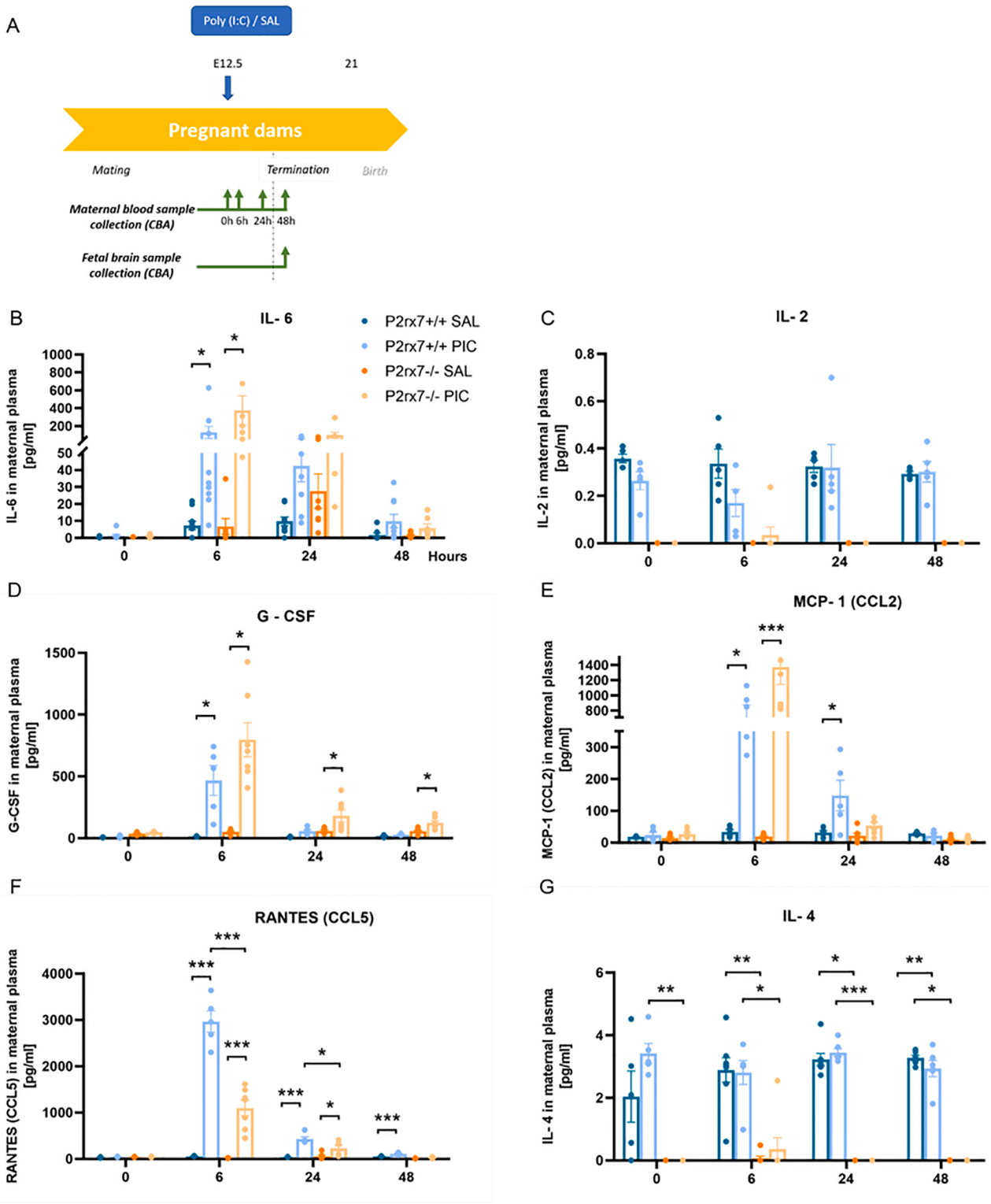

Fig. 6. Cytokine and chemokine concentrations measured in maternal plasma samples at different time points following poly(I:C) administration. (A) The experimental protocol shown in a flowchart *(Experiment 2)*. Prior to terminal blood collection and 48-hour fetal brain collection, blood was collected at the above three time points from 5 to 10 pregnant animals per group, collecting 1–3 fetal brains of similar appearance and different uterine positions per animal. (B) IL-6 concentrations were elevated in both P2rx7$^{+/+}$ and P2rx7$^{-/-}$ plasma samples following poly(I:C) injection. (C) No significant difference appeared between saline and PIC groups in maternal plasma of IL-2. (D) G-CSF was elevated in both P2rx7$^{+/+}$ and P2rx7$^{-/-}$ PIC treated animal samples in maternal plasma in the 6th hour and showed higher values in plasma in all knockout groups. (E-F) Plasma levels of chemokines increased after PIC treatment. RANTES plasma levels (F) were significantly lower in the P2X7-deficient PIC-treated group than in the wild-type counterpart. IL-4 plasma concentrations (G) showed higher values in wild-type groups but were not induced by PIC. Cytokine and chemokine values measured in the fetal brains are expressed in picograms per total protein. All data are expressed as mean ± s.e.m. Statistical tests used with exact n, F, and p values are provided in *Supplementary Table*. *$p < 0.05$. **$p < 0.01$. ***$p < 0.001$.

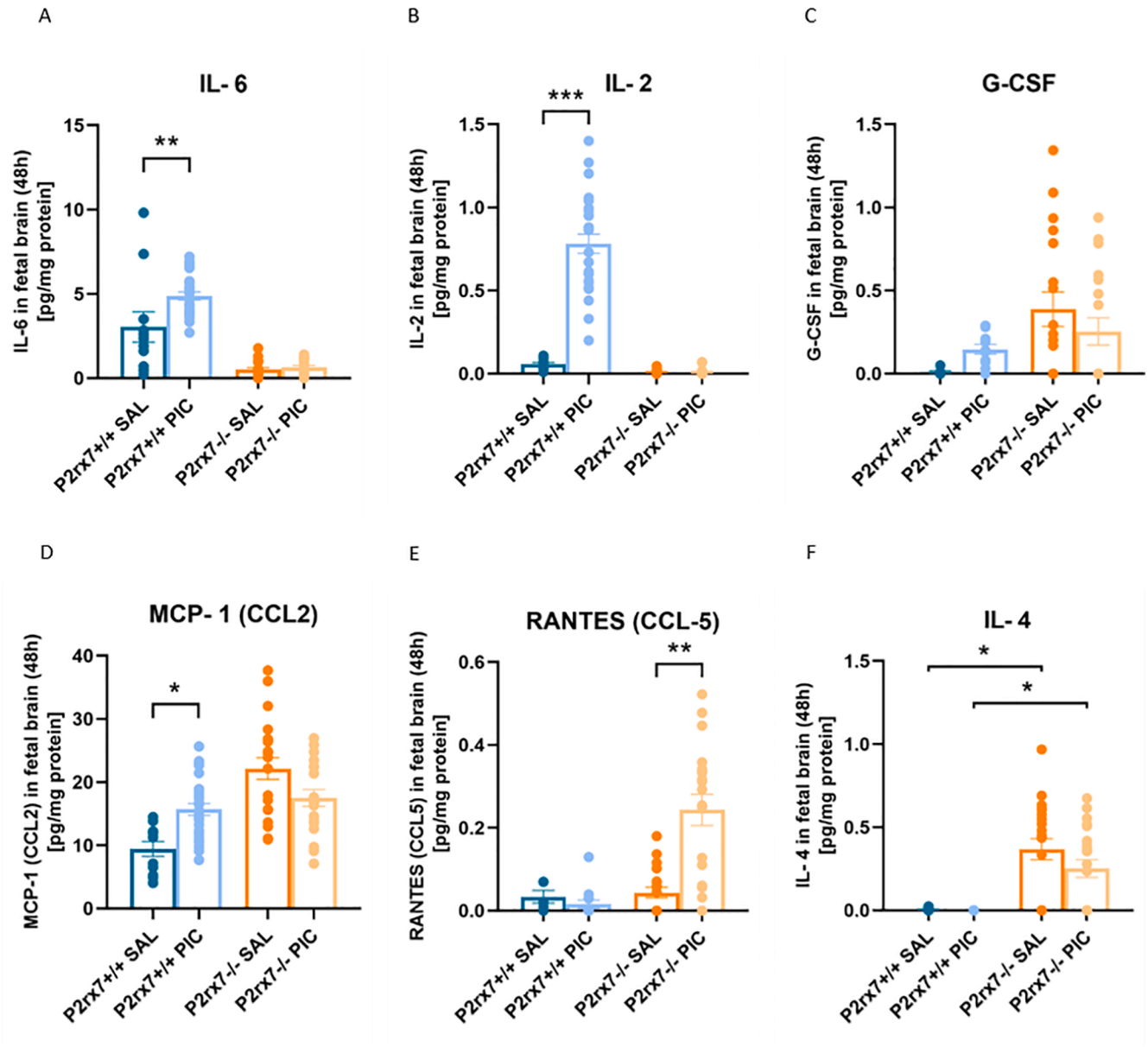

Fig. 7. Cytokine and chemokine concentrations measured in fetal brain samples at 48 h following maternal immune activation. Fetal brain samples were collected 48 h after MIA induction, along with terminal maternal blood sampling. (A-B) In fetal brain, the lack of P2X7 receptors prevented the increase in IL-6 (A) and IL-2 (B) levels caused by PIC treatment. (C) G-CSF was not significantly induced in fetal brain. (D) MCP-1 was induced by MIA, and the lack of P2X7 prevented this effect. (E) RANTES showed outstanding concentration values in the P2rx7-deficient group. (F) Anti-inflammatory IL-4 levels of $P2rx7^{-/-}$ groups showed increased values in fetal brain compared to $P2rx7^{+/+}$ counterparts on the contrary with its plasma level. Cytokine and chemokine values measured in the fetal brains are expressed in picograms per total protein. All data are expressed as mean ± s.e.m. Statistical tests used with exact n, F, and p values are provided in *Supplementary Table.* $^{*}p < 0.05$. $^{**}p < 0.01$. $^{***}p < 0.001$.

expression in a subsequent P2X7-independent process.

RANTES (CCL5) and MCP-1 (CCL2) are chemotactic cytokines that play role in recruiting and attracting leukocytes into inflammatory sites. In our experiments, both MCP-1′ and RANTES′ peak concentration in maternal plasma occurred 6 h after poly(I:C) treatment and then displayed a gradual decrease by 48 h. With robust elevation in poly(I:C)-induced plasma RANTES concentration of $P2rx7^{+/+}$ samples and a significantly lower increase in $P2rx7^{-/-}$ samples, the cytokine response is a partially genotype-dependent mechanism. Although RANTES elevation occurs in the absence of P2X7 in plasma, the mean concentrations are half as high as in the presence of P2X7, so the receptor may play a role in the development of the complete RANTES response upon immune activation. P2X7 receptors also play a role in the induction of plasma MCP-1 levels 24 h, but not 6 h following poly(I:C) treatment indicating that in the absence of P2X7, MCP-1 induction subsides earlier. G-CSF is known as a growth factor for neurons and neural stem cells and stimulates neurogenesis (Wallner et al., 2015), plays a protective role in response to nerve injury, and has anti-apoptotic activity (Schneider et al., 2005). We found a significant increase in G-CSF concentration of maternal plasma at 6 h following MIA, gradually decreasing by 48 h in $P2rx7^{+/+}$ samples and an even longer-term elevation in the $P2rx7^{-/-}$ group which may mean that in the absence of P2X7, a compensatory G-CSF response was elicited by poly(I:C) to replace P2X7-mediated mechanisms.

Fetal brain IL-1β at 24 h and IL-2, IL-6, and MCP-1 (CCL2) concentration at 48 h all showed a P2X7-dependent increase, although, for MCP-1, $P2rx7^{-/-}$ condition alone showed higher cytokine levels. While several signaling processes in maternal plasma can lead to an increase in

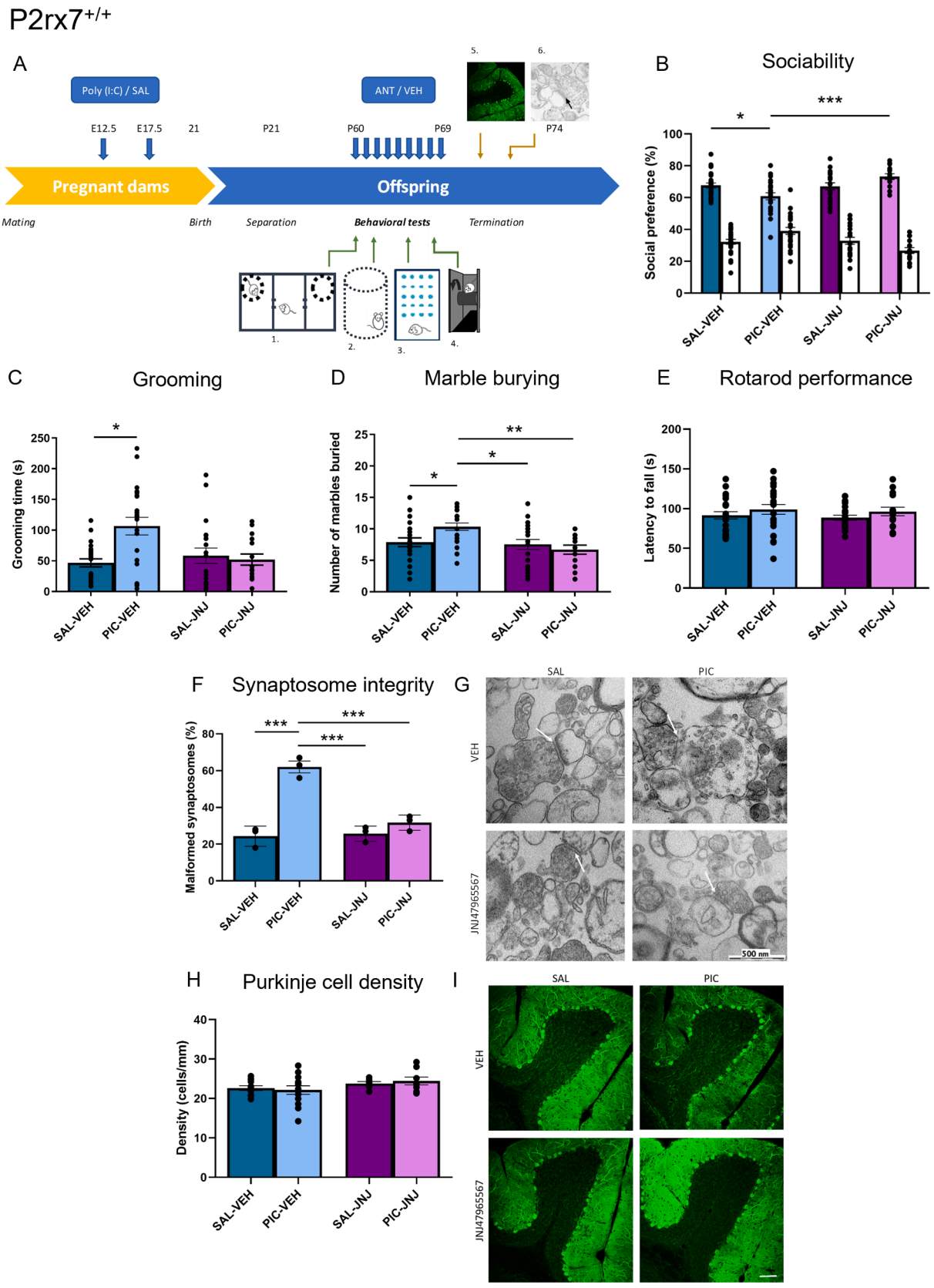

Fig. 8. Repetitive offspring treatment with P2X7 antagonist (JNJ47965567) prevented MIA-induced effects in P2rx7$^{+/+}$ mice. (A) The experimental protocol shown in a flowchart *(Experiment 3)*. (B-D) Changes in behavioral tests during subchronic antagonist treatment were examined. Antagonist treatment averted social deficit (B) and normalized repetitive behaviours (C-D). (E) MIA did not influence sensorimotor coordination. (F-G) MIA increased the number of malformed synaptosomes in the control group, which was prevented in the antagonist-treated group. Scale bar 500 nm. (H-I) MIA had no influence on Purkinje cell number, which is consistent with the result of sensorimotor coordination test. Scale bar 100 μm. All data are expressed as mean ± s.e.m. Statistical tests used with exact n, F, and p values are provided in *Supplementary Table.* *$p < 0.05$. **$p < 0.01$. ***$p < 0.001$.

IL-6, a specific P2X7-dependent mechanism can be hypothesized in the fetal brain. These results show that P2X7 plays a significant role in fetal brain alterations of cytokine levels, which may be associated with the observed behavioral and morphological abnormalities.

In contrast to its plasma levels, in fetal brain, RANTES concentration did not increase by MIA in the presence of P2X7, whereas it did in the absence. Thus, it is conceivable that this increase was a compensatory reaction to replace one of the P2X7-mediated processes. Further research is needed to clarify the precise and time-dependent relationship between different inflammatory mediators in the fetal brain and to identify the role of these mediators in the development and maturation of offspring brain and subsequent behavioral alterations.

Activation of P2X7 leads to NLRP3 inflammasome activation and subsequent IL-1β secretion (Karmakar et al., 2016; MacKenzie et al., 2001). Since NLRP3 seemed to be involved in the offspring's response to MIA, therefore it was worthwhile to investigate the potential role of IL-1β. We found that maternal poly(I:C) induced phenotype was absent after maternal administration of IL-1β neutralizing antibody and in IL-1β KO animals (*see Supplementary*). These results imply IL-1β is required for the development of autistic features in mice.

Similarly to the result of Arrode-Brusés and Brusés (Arrode-Brusés and Brusés, 2012), we found elevated IL-1β levels shortly after MIA induction in maternal plasma and 24 h after the injection in fetal brain and placenta, which suggests early maternal cytokine production has a delayed effect on the developing fetal brain. Poly(I:C) did not affect the IL-1β concentration significantly in maternal plasma of P2rx7 knockout or JNJ47965567 treated mice, but a tendency of elevation after MIA was visible. Thus, in the case of maternal plasma, the increase in IL-1β concentration does not appear to be dependent on the P2X7 receptor. However, in placental and fetal brain samples of the same groups, we found equally lower levels of IL-1β indicating that poly(I:C) induced IL-1β production is a P2X7-dependent mechanism in the offspring. This is consistent with the role of IL-1β in shaping poly(I:C) induced offspring behavior.

In addition, the plasma of NLRP3 inhibited dams showed an elevated amount of IL-1β similar to the saline-pretreated poly(I:C) group suggesting that early IL-1β production induced by maternal immune activation in maternal plasma was an NLRP3-independent mechanism. We further found that NLRP3 antagonism alone was sufficient to prevent IL-1β elevation in fetal brain, confirming our hypothesis that the NLRP3 protein plays a role in mediating P2X7-induced processes. Comparing the increase in IL-1β in maternal plasma, there was no increase in fetal brain and placenta in the MCC950-treated groups in contrast to the control groups, suggesting that maternal cytokines do not cross placental barrier in large amounts. Another group also found only a minimal amount of maternally produced IL-1β crossing the placental barrier, upon inflammatory challenge (Girard and Sebire, 2016). Since the placenta is known to express TLR3 (Bryant et al., 2017; Pudney et al., 2016), we suggest that elevated IL-1β measured in the placenta and fetal brain was mostly induced locally through TLR3-P2X7-NLRP3 signaling

Another aim was to demonstrate the effects of repeated P2X7 antagonist treatment and verify P2X7 as a potential therapeutic target. JNJ47965567 is a high-affinity, selective CNS permeable P2X7 antagonist (Bhattacharya et al., 2013), which has been proven effective in animal models of other psychiatric disorders, such as depression (Bhattacharya and Ceusters, 2020) and schizophrenia (Koványi et al., 2016). Importantly, P2X7 antagonists are under phase II clinical trial as potential antidepressant agents (Antidepressant Trial With P2X7 Antagonist JNJ-54175446, ClinicalTrials.gov/NCT04116606, 2019) and have emerged as promising upstream regulators of anti-inflammatory strategies in neuropsychopharmacology. In our current study, repeated administration of a lower dose of JNJ47965567 reversed autism-like phenotype in offspring of poly(I:C) treated dams. This confirmed our previous experiment with a single-dose protocol of a higher dose in a manner more closely resembling a potential human treatment regime. Interestingly, we did not detect sensorimotor coordination impairment and Purkinje cell loss in offspring in response to MIA in this series of experiments with JNJ47965567 treatments. One possible explanation for the partial loss of phenotype is the potential variance amongst different poly(I:C) batches. Mounting evidence shows poly(I:C) products can vary in terms of their immunogenicity between different batches and can induce varying immune responses, pregnancy outcomes, and phenotypes (Kowash et al., 2019; Mueller et al., 2019; Vigli et al., 2020). Another potential confounder is that offspring were subjected to repeated daily i.p. injections before and during behavior tests for five days, which might have affected motor performance and overshadowed the mild effect of maternal poly(I:C) treatment.

Repeated treatment with JNJ47965567 neutralized the pathological effect of MIA on synapse integrity in offspring. Hence repeated progeny treatment reversed morphological abnormalities that have already developed, suggesting P2X7 activation may also play an important role in maintaining persistent autism-like abnormalities resulting from MIA. In other animal and human autism studies, a non-selective P2 receptor antagonist suramin has been shown to be effective (Naviaux, 2018; Naviaux et al., 2017). Altogether, it appears that centrally permeable, high-affinity, selective P2X7 antagonists, such as JNJ47965567 may prove to be potential pharmacological agents for ASD therapy. However, a number of additional experiments are needed to determine whether it is effective in keeping the autistic behaviours under control or as a longer-term therapy.

In conclusion, we demonstrated that NLRP3 is a likely mediator of P2X7 activation following MIA in mice and may serve as a therapeutic target in ASD. In addition, we obtained a time-dependent insight to poly (I:C)-induced cytokine and chemokine response, which highlighted further mediators potentially involved in MIA-induced, P2X7-mediated long-term impact on brain development. Such important mediators could be RANTES and MCP-1 in the maternal circulation and IL-1β, IL-6, IL-2, and MCP-1 in the fetal brain. Finally, we showed that repeated treatment of P2X7 antagonist is effective in reducing autistic features.

Funding and disclosure

This work was supported by the Hungarian Research and Development Fund [grant number 131629], Hungarian Brain Research Program [2017-1.2.1-NKP-2017-00002 to B.S.], the European Union's Horizon 2020 Research and Innovation Programme under the Marie Skłodowska Curie grant agreement No. 766124 and the Gedeon Richter plc. D.SZ is a recipient of a Gedeon Richter PhD fellowship.

Declaration of Competing Interest

The authors declare that they have no known competing financial interests or personal relationships that could have appeared to influence the work reported in this paper.

Acknowledgments

The authors are grateful to Kornél Demeter at the Behavioral Unit of IEM for providing technical support and assisting in the behavioral experiments, and the support of the Cell Biology Center (Flow Cytometry Core Facility), and the Nikon Microscopy Center of IEM.

Appendix A. Supplementary data

Supplementary data to this article can be found online at https://doi.org/10.1016/j.bbi.2022.01.015.

References

Antidepressant Trial With P2X7 Antagonist JNJ-54175446. https://ClinicalTrials.gov/show/NCT04116606.

Adhikari, A., Xu, M., Chen, Z.J., 2007. Ubiquitin-mediated activation of TAK1 and IKK. Oncogene 26 (22), 3214–3226. https://doi.org/10.1038/sj.onc.1210413.

American Psychiatric Association, A.P.A.D.S.M.T.F., 2017. Diagnostic and statistical manual of mental disorders : DSM-5. American Psychiatric Association, Arlington, VA.

Arrode-Brusés, G., Brusés, J.L., 2012. Maternal immune activation by poly I: C induces expression of cytokines IL-1β and IL-13, chemokine MCP-1 and colony stimulating factor VEGF in fetal mouse brain. J. Neuroinflamm. 9, 83. https://doi.org/10.1186/1742-2094-9-83.

Ashwood, P., Krakowiak, P., Hertz-Picciotto, I., Hansen, R., Pessah, I., Van de Water, J., 2011a. Elevated plasma cytokines in autism spectrum disorders provide evidence of immune dysfunction and are associated with impaired behavioral outcome. Brain Behav, Immun, 25 (1), 40–45. https://doi.org/10.1016/j.bbi.2010.08.003.

Ashwood, P., Krakowiak, P., Hertz-Picciotto, I., Hansen, R., Pessah, I.N., Van de Water, J., 2011b. Associations of impaired behaviors with elevated plasma chemokines in autism spectrum disorders. J. Neuroimmunol. 232 (1-2), 196–199. https://doi.org/10.1016/j.jneuroim.2010.10.025.

Bartlett, R., Stokes, L., Sluyter, R., Sibley, D.R., 2014. The P2X7 receptor channel: recent developments and the use of P2X7 antagonists in models of disease. Pharmacol. Rev. 66 (3), 638–675. https://doi.org/10.1124/pr.113.008003.

Bhattacharya, A., Ceusters, M., 2020. Targeting neuroinflammation with brain penetrant P2X7 antagonists as novel therapeutics for neuropsychiatric disorders. Neuropsychopharmacology 45 (1), 234–235. https://doi.org/10.1038/s41386-019-0502-9.

Bhattacharya, A., Wang, Q.i., Ao, H., Shoblock, J.R., Lord, B., Aluisio, L., Fraser, I., Nepomuceno, D., Neff, R.A., Welty, N., Lovenberg, T.W., Bonaventure, P., Wickenden, A.D., Letavic, M.A., 2013. Pharmacological characterization of a novel centrally permeable P2X7 receptor antagonist: JNJ-47965567. Br. J. Pharmacol. 170 (3), 624–640. https://doi.org/10.1111/bph.12314.

Bryant, A.H., Menzies, G.E., Scott, L.M., et al., 2017. Human gestation-associated tissues express functional cytosolic nucleic acid sensing pattern recognition receptors. Clin. Exp. Immunol. 189, 36-46 10.1111/cei.12960.

Buehler., M.R., 2011. A proposed mechanism for autism: an aberrant neuroimmune response manifested as a psychiatric disorder. Med. Hypotheses. 76, 863-870.

Burns, K., Martinon, F., Tschopp, J., 2003. New insights into the mechanism of IL-1beta maturation. Curr. Opin. Immunol. 15, 26–30. https://doi.org/10.1016/s0952-7915(02)00017-1.

Di Virgilio, F., Dal Ben, D., Sarti, A.C., Giuliani, A.L., Falzoni, S., 2017. The P2X7 receptor in infection and inflammation. Immunity 47 (1), 15–31. https://doi.org/10.1016/j.immuni.2017.06.020.

Dinarello, C.A., 2005. Blocking IL-1 in systemic inflammation. J. Exp. Med. 201, 1355–1359. https://doi.org/10.1084/jem.20050640.

Ermolaeva, M.A., Michallet, M.-C., Papadopoulou, N., Utermöhlen, O., Kranidioti, K., Kollias, G., Tschopp, J., Pasparakis, M., 2008. Function of TRADD in tumor necrosis factor receptor 1 signaling and in TRIF-dependent inflammatory responses. Nat. Immunol. 9 (9), 1037–1046. https://doi.org/10.1038/ni.1638.

Estes, M.L., Prendergast, K., MacMahon, J.A., Cameron, S., Aboubechara, J.P., Farrelly, K., Sell, G.L., Haapanen, L., Schauer, J.D., Horta, A., Shaffer, I.C., Le, C.T., Kincheloe, G.N., Tan, D.J., van der List, D., Bauman, M.D., Carter, C.S., Van de Water, J., McAllister, A.K., 2020. Baseline immunoreactivity before pregnancy and poly(I:C) dose combine to dictate susceptibility and resilience of offspring to maternal immune activation. Brain Behav. Immun. 88, 619–630. https://doi.org/10.1016/j.bbi.2020.04.061.

Gardener, H., Spiegelman, D., Buka, S.L., 2009. Prenatal risk factors for autism: comprehensive meta-analysis. Br. J. Psychiatry 195 (1), 7–14. https://doi.org/10.1192/bjp.bp.108.051672.

Garré, J.M., Silva, H.M., Lafaille, J.J., Yang, G., 2020. P2X7 receptor inhibition ameliorates dendritic spine pathology and social behavioral deficits in Rett syndrome mice. Nat. Commun. 11 (1) https://doi.org/10.1038/s41467-020-15590-5.

Girard, S., Sebire, G., 2016. Transplacental transfer of interleukin-1 receptor agonist and antagonist following maternal immune activation. Am. J. Reprod. Immunol. 75 (1), 8–12. https://doi.org/10.1111/aji.12444.

Goines, P.E., Croen, L.A., Braunschweig, D., Yoshida, C.K., Grether, J., Hansen, R., Kharrazi, M., Ashwood, P., Van de Water, J., 2011. Increased midgestational IFN-γ, IL-4 and IL-5 in women bearing a child with autism: a case-control study. Mol. Autism 2 (1). https://doi.org/10.1186/2040-2392-2-13.

Hashimoto, T., Tayama, M., Murakawa, K., Yoshimoto, T., Miyazaki, M., Harada, M., Kuroda, Y., 1995. Development of the brainstem and cerebellum in autistic patients. J. Autism Dev. Disord. 25 (1), 1–18. https://doi.org/10.1007/BF02178163.

He, Y., Hara, H., Núñez, G., 2016. Mechanism and regulation of NLRP3 inflammasome activation. Trends Biochem. Sci. 41 (12), 1012–1021. https://doi.org/10.1016/j.tibs.2016.09.002.

Hirota, S.A., Ng, J., Lueng, A., Khajah, M., Parhar, K., Li, Y., Lam, V., Potentier, M.S., Ng, K., Bawa, M., McCafferty, D.-M., Rioux, K.P., Ghosh, S., Xavier, R.J., Colgan, S. P., Tschopp, J., Muruve, D., MacDonald, J.A., Beck, P.L., 2011. NLRP3 inflammasome plays a key role in the regulation of intestinal homeostasis. Inflamm. Bowel Dis. 17 (6), 1359–1372. https://doi.org/10.1002/ibd.21478.

Horai, R., Asano, M., Sudo, K., et al., 1998. Production of mice deficient in genes for interleukin (IL)-1alpha, IL-1beta, IL-1alpha/beta, and IL-1 receptor antagonist shows that IL-1beta is crucial in turpentine-induced fever development and glucocorticoid secretion. J. Exp. Med. 187, 1463–1475. https://doi.org/10.1084/jem.187.9.1463.

Horváth, G., Otrokocsi, L., Beko, K., et al., 2019. P2X7 Receptors drive Poly(I:C) induced autism-like behavior in mice. J. Neurosci. 39, 2542-2561 10.1523/jneurosci.1895-18.2019.

Hughes, H.K., Rose, D., Ashwood, P., 2018. The gut microbiota and dysbiosis in autism spectrum disorders. Curr. Neurol Neurosci. Rep. 18, 81. https://doi.org/10.1007/s11910-018-0887-6.

Jiang, H.-Y., Xu, L.-L., Shao, L.i., Xia, R.-M., Yu, Z.-h., Ling, Z.-X., Yang, F., Deng, M., Ruan, B., 2016. Maternal infection during pregnancy and risk of autism spectrum disorders: A systematic review and meta-analysis. Brain Behav. Immun. 58, 165–172. https://doi.org/10.1016/j.bbi.2016.06.005.

Jones, K.L., Croen, L.A., Yoshida, C.K., Heuer, L., Hansen, R., Zerbo, O., DeLorenze, G.N., Kharrazi, M., Yolken, R., Ashwood, P., Van de Water, J., 2017. Autism with intellectual disability is associated with increased levels of maternal cytokines and chemokines during gestation. Mol. Psychiatry 22 (2), 273–279. https://doi.org/10.1038/mp.2016.77.

Kanneganti, T.-D., Lamkanfi, M., Kim, Y.-G., Chen, G., Park, J.-H., Franchi, L., Vandenabeele, P., Núñez, G., 2007. Pannexin-1-mediated recognition of bacterial molecules activates the cryopyrin inflammasome independent of Toll-like receptor signaling. Immunity 26 (4), 433–443. https://doi.org/10.1016/j.immuni.2007.03.008.

Kanneganti, T.-D., Lamkanfi, M., Núñez, G., 2007. Intracellular NOD-like receptors in host defense and disease. Immunity 27 (4), 549–559. https://doi.org/10.1016/j.immuni.2007.10.002.

Karmakar, M., Katsnelson, M.A., Dubyak, G.R., Pearlman, E., 2016. Neutrophil P2X7 receptors mediate NLRP3 inflammasome-dependent IL-1β secretion in response to ATP. Nat. Commun. 7 (1) https://doi.org/10.1038/ncomms10555.

Koványi, B., Csölle, C., Calovi, S., Hanuska, A., Kató, E., Köles, L., Bhattacharya, A., Haller, J., Sperlágh, B., 2016. The role of P2X7 receptors in a rodent PCP-induced schizophrenia model. Sci. Rep. 6 (1) https://doi.org/10.1038/srep36680.

Kowash, H.M., Potter, H.G., Edye, M.E., Prinssen, E.P., Bandinelli, S., Neill, J.C., Hager, R., Glazier, J.D., 2019. Poly(I:C) source, molecular weight and endotoxin contamination affect dam and prenatal outcomes, implications for models of maternal immune activation. Brain Behav. Immun. 82, 160–166. https://doi.org/10.1016/j.bbi.2019.08.006.

Kofalvi, A., Vizi, E.S., Ledent, C., Sperlagh, B., 2003. Cannabinoids inhibit the release of [3H]glutamate from rodent hippocampal synaptosomes via a novel CB1 receptor-independent action. Eur. J. Neurosci. 18 (7), 1973–1978. https://doi.org/10.1046/j.1460-9568.2003.02897.x.

Kyzar, E., Gaikwad, S., Roth, A., Green, J., Pham, M., Stewart, A., Liang, Y., Kobla, V., Kalueff, A.V., 2011. Towards high-throughput phenotyping of complex patterned behaviors in rodents: focus on mouse self-grooming and its sequencing. Behav. Brain Res. 225 (2), 426–431. https://doi.org/10.1016/j.bbr.2011.07.052.

Lamkanfi, M., Kanneganti, T.-D., Franchi, L., Núñez, G., 2007. Caspase-1 inflammasomes in infection and inflammation. J. Leukoc. Biol. 82 (2), 220–225. https://doi.org/10.1189/jlb.1206756.

Li, X., Chauhan, A., Sheikh, A.M., Patil, S., Chauhan, V., Li, X.-M., Ji, L., Brown, T., Malik, M., 2009. Elevated immune response in the brain of autistic patients. J. Neuroimmunol. 207 (1-2), 111–116. https://doi.org/10.1016/j.jneuroim.2008.12.002.

Lyall, K., Ashwood, P., Van de Water, J., et al., 2014. Maternal immune-mediated conditions, autism spectrum disorders, and developmental delay. J. Autism Dev. Disord. 44, 1546–1555. https://doi.org/10.1007/s10803-013-2017-2.

MacKenzie, A., Wilson, H.L., Kiss-Toth, E., et al., 2001. Rapid secretion of interleukin-1beta by microvesicle shedding. Immunity 15, 825–835. https://doi.org/10.1016/s1074-7613(01)00229-1.

Maenner, M.J., Shaw, K.A., Baio, J., et al., 2020. Prevalence of Autism Spectrum Disorder Among Children Aged 8 Years - Autism and Developmental Disabilities Monitoring Network, 11 Sites, United States, 2016. MMWR Surveill Summ 69, 1-12 10.15585/mmwr.ss6904a1.

Malkova, N.V., Yu, C.Z., Hsiao, E.Y., Moore, M.J., Patterson, P.H., 2012. Maternal immune activation yields offspring displaying mouse versions of the three core symptoms of autism. Brain Behav. Immun. 26 (4), 607–616. https://doi.org/10.1016/j.bbi.2012.01.011.

Mariathasan, S., Weiss, D.S., Newton, K., McBride, J., O'Rourke, K., Roose-Girma, M., Lee, W.P., Weinrauch, Y., Monack, D.M., Dixit, V.M., 2006. Cryopyrin activates the inflammasome in response to toxins and ATP. Nature 440 (7081), 228–232. https://doi.org/10.1038/nature04515.

Martinon, F., Burns, K., Tschopp, J., 2002. The inflammasome: a molecular platform triggering activation of inflammatory caspases and processing of proIL-beta. Mol. Cell 10 (2), 417–426.

Masi, A., Quintana, D.S., Glozier, N., Lloyd, A.R., Hickie, I.B., Guastella, A.J., 2015. Cytokine aberrations in autism spectrum disorder: a systematic review and meta-analysis. Mol. Psychiatry 20 (4), 440–446. https://doi.org/10.1038/mp.2014.59.

Motulsky, H.J., Brown, R.E., 2006. Detecting outliers when fitting data with nonlinear regression - a new method based on robust nonlinear regression and the false discovery rate. BMC Bioinf. 7, 123. https://doi.org/10.1186/1471-2105-7-123.

Mueller, F.S., Richetto, J., Hayes, L.N., Zambon, A., Pollak, D.D., Sawa, A., Meyer, U., Weber-Stadlbauer, U., 2019. Influence of poly(I:C) variability on thermoregulation, immune responses and pregnancy outcomes in mouse models of maternal immune activation. Brain Behav. Immun. 80, 406–418. https://doi.org/10.1016/j.bbi.2019.04.019.

Naviaux, R.K., 2018. Antipurinergic therapy for autism-An in-depth review. Mitochondrion 43, 1–15. https://doi.org/10.1016/j.mito.2017.12.007.

Naviaux, R.K., Curtis, B., Li, K., Naviaux, J.C., Bright, A.T., Reiner, G.E., Westerfield, M., Goh, S., Alaynick, W.A., Wang, L., Capparelli, E.V., Adams, C., Sun, J.i., Jain, S., He, F., Arellano, D.A., Mash, L.E., Chukoskie, L., Lincoln, A., Townsend, J., 2017. Low-dose suramin in autism spectrum disorder: a small, phase I/II, randomized clinical trial. Ann. Clin. Transl. Neurol. 4 (7), 491–505. https://doi.org/10.1002/acn3.424.

Naviaux, R.K., Zolkipli, Z., Wang, L., Nakayama, T., Naviaux, J.C., Le, T.P., Schuchbauer, M.A., Rogac, M., Tang, Q., Dugan, L.L., Powell, S.B., Lakshmana, M.K.,

2013. Antipurinergic therapy corrects the autism-like features in the poly(IC) mouse model. PLoS ONE 8 (3), e57380. https://doi.org/10.1371/journal.pone.0057380.
Pellegrini, C., Antonioli, L., Calderone, V., Colucci, R., Fornai, M., Blandizzi, C., 2020. Microbiota-gut-brain axis in health and disease: Is NLRP3 inflammasome at the crossroads of microbiota-gut-brain communications? Prog. Neurobiol. 191, 101806. https://doi.org/10.1016/j.pneurobio.2020.101806.
Persico, A.M., Ricciardello, A., Cucinotta, F., 2019. The psychopharmacology of autism spectrum disorder and Rett syndrome. Handb. Clin. Neurol. 165, 391–414. https://doi.org/10.1016/b978-0-444-64012-3.00024-1.
Pirhonen, J., Sareneva, T., Kurimoto, M., et al., 1999. Virus infection activates IL-1 beta and IL-18 production in human macrophages by a caspase-1-dependent pathway. J. Immunol. 162, 7322–7329.
Pudney, J., He, X., Masheeb, Z., Kindelberger, D.W., Kuohung, W., Ingalls, R.R., 2016. Differential expression of toll-like receptors in the human placenta across early gestation. Placenta 46, 1–10. https://doi.org/10.1016/j.placenta.2016.07.005.
Saresella, M., Piancone, F., Marventano, I., Zoppis, M., Hernis, A., Zanette, M., Trabattoni, D., Chiappedi, M., Ghezzo, A., Canevini, M.P., la Rosa, F., Esposito, S., Clerici, M., 2016. Multiple inflammasome complexes are activated in autistic spectrum disorders. Brain Behav. Immun. 57, 125–133. https://doi.org/10.1016/j.bbi.2016.03.009.
Schneider, A., Kuhn, H.G., Schäbitz, W.R., 2005. A role for G-CSF (granulocyte-colony stimulating factor) in the central nervous system. Cell Cycle 4, 1753–1757. https://doi.org/10.4161/cc.4.12.2213.
Smith, S.E.P., Li, J., Garbett, K., Mirnics, K., Patterson, P.H., 2007. Maternal immune activation alters fetal brain development through interleukin-6. J. Neurosci. 27 (40), 10695–10702.
Solle, M., Labasi, J., Perregaux, D.G., Stam, E., Petrushova, N., Koller, B.H., Griffiths, R. J., Gabel, C.A., 2001. Altered cytokine production in mice lacking P2X(7) receptors. J. Biol. Chem. 276 (1), 125–132. https://doi.org/10.1074/jbc.M006781200.
Sperlágh, B., Illes, P., 2014. P2X7 receptor: an emerging target in central nervous system diseases. Trends Pharmacol. Sci. 35 (10), 537–547. https://doi.org/10.1016/j.tips.2014.08.002.
Sutterwala, F.S., Ogura, Y., Zamboni, D.S., Roy, C.R., Flavell, R.A., 2006. NALP3: a key player in caspase-1 activation. J. Endotoxin Res. 12 (4), 251–256.
Thomas, P.G., Dash, P., Aldridge, J.R., Ellebedy, A.H., Reynolds, C., Funk, A.J., Martin, W.J., Lamkanfi, M., Webby, R.J., Boyd, K.L., Doherty, P.C., Kanneganti, T.-D., 2009. The intracellular sensor NLRP3 mediates key innate and healing responses to influenza A virus via the regulation of caspase-1. Immunity 30 (4), 566–575. https://doi.org/10.1016/j.immuni.2009.02.006.
Vigli, D., Palombelli, G., Fanelli, S., Calamandrei, G., Canese, R., Mosca, L., Scattoni, M. L., Ricceri, L., 2020. Maternal immune activation in mice only partially recapitulates the autism spectrum disorders symptomatology. Neuroscience 445, 109–119.
Wallner, S., Peters, S., Pitzer, C., Resch, H., Bogdahn, U., Schneider, A., 2015. The Granulocyte-colony stimulating factor has a dual role in neuronal and vascular plasticity. Front. Cell Dev. Biol. 3 https://doi.org/10.3389/fcell.2015.00048.
Wei, H., Alberts, I., Li, X., 2013. Brain IL-6 and autism. Neuroscience 252, 320–325. https://doi.org/10.1016/j.neuroscience.2013.08.025.
Wong, H., Hoeffer, C., 2018. Maternal IL-17A in autism. Exp. Neurol. 299, 228–240. https://doi.org/10.1016/j.expneurol.2017.04.010.
Wu, S., Ding, Y., Wu, F., Li, R., Xie, G., Hou, J., Mao, P., 2015. Family history of autoimmune diseases is associated with an increased risk of autism in children: A systematic review and meta-analysis. Neurosci. Biobehav. Rev. 55, 322–332. https://doi.org/10.1016/j.neubiorev.2015.05.004.
Wu, W.-L., Hsiao, E.Y., Yan, Z., Mazmanian, S.K., Patterson, P.H., 2017. The placental interleukin-6 signaling controls fetal brain development and behavior. Brain Behav. Immun. 62, 11–23. https://doi.org/10.1016/j.bbi.2016.11.007.
Xu, N., Li, X., Zhong, Y., 2015. Inflammatory cytokines: potential biomarkers of immunologic dysfunction in autism spectrum disorders. Mediators Inflamm. 2015, 1–10. https://doi.org/10.1155/2015/531518.
Yang, Y., Wang, H., Kouadir, M., Song, H., Shi, F., 2019. Recent advances in the mechanisms of NLRP3 inflammasome activation and its inhibitors. Cell Death Dis. 10 (2) https://doi.org/10.1038/s41419-019-1413-8.
Zaretsky, M.V., Alexander, J.M., Byrd, W., Bawdon, R.E., 2004. Transfer of inflammatory cytokines across the placenta. Obstet. Gynecol. 103 (3), 546–550.